ELSEVIER

A new estimation method of irradiance on a partially shaded PV generator in grid-connected photovoltaic systems

M. Drif[a,b,*], P.J. Pérez[a], J. Aguilera[a], J.D. Aguilar[a]

[a]Grupo de Investigación IDEA, Departamento de Electrónica, Escuela Politécnica Superior, Universidad de Jaén, Campus Las Lagunillas, 23071 Jaén, Spain
[b]Centre de Développement des Energies Renouvelables, BP 62, Route de l'Observatoire, 16340 Bouzaréah, Algiers, Algeria

Abstract

A new method for estimating the irradiance on a partially shaded photovoltaic generator system is proposed. The basic principle of this method consists of two parts: firstly, an approximation of the obstacles' outline or the local horizon by a set of linear functions. Here, a survey of the surroundings is based on the reading of the topographic coordinates of the only significant points of all the objects surrounding the photovoltaic generator. Secondly, the irradiance on the photovoltaic plane is estimated using an accurate model such as the Perez et al. model and assuming that the shading affects both the direct radiation and a part of the diffuse component (circumsolar component).

The aim of this paper is to present the principles of the proposed method and the algorithm used for calculating the irradiance on shaded planes. In addition, the results of the comparison between the simulated and measured values of this method are presented.
© 2007 Elsevier Ltd. All rights reserved.

Keywords: Grid-connected PV system; Irradiance on tilted planes; Partial shading; Shading factor; Obstacles' outline

1. Introduction

Today, grid-connected building integrated photovoltaic (GC-BIPV) systems are becoming a popular feature in the built environment in many of the developed countries. This system forms an integral part of the urban edifices such as: envelopes, rooftops, pergolas, shading devices, etc.

As of end 2004, a cumulative total of more than 2.6 GW of PV have been installed in IEA-PVPS participating countries, with annual growth rates between 20% in 1994 and over 42% in 2004 [1]. Among these, grid-connected (GC) system applications had the highest portion with over 93% of the capacity installed in 2004. The motivation in building integrated photovoltaic (BIPV) systems could be driven from the large potential for cost reduction and can contribute to the building aesthetics. However, a BIPV system is often subjected to shading problems caused by surrounding obstructions of irregular geometries such as trees, overhangs, chimney, telephone poles, other buildings, etc. Such shading phenomena can cause two principal effects: extrinsically, it leads to reduction of incident solar irradiance and consequently a reduction in power production, and intrinsically, the inhomogeneous irradiance on the PV surface may cause electrical mismatch and hot spots.

In a large number of BIPV systems in the European Union (EU), shading caused annual yield reductions between 5% and 10% [2]. As an indication, in the German 1000 Roofs Programme, it was recorded that 41% of the installed systems were affected by shading, which represents a 10% energy loss [3]. The same results have been found in the Japanese field test programme [3].

One of the crucial parameters required for estimating the energy production, and therefore the performance yield of GC-BIPV systems in urban areas, is the solar radiation received on the plane of the photovoltaic generator. Knowledge of this parameter enables accurate calculations of shading effects to be done. In this sense, several methods

*Corresponding author at: Centre de Developpement des Energies Renouvelables, BP 62, Route de l'Observatoire, 16340 Bouzareah, Algiers, Algeria. Tel.: +213 79 29 39 16/+34 953212347; fax: +34 953211967.

E-mail addresses: m_drif@hotmail.com, mahmoud@ujaen.es (M. Drif).

Nomenclature

B_h	direct irradiance on a horizontal plane, W/m^2
B_t	direct irradiance on the PV generator plane, W/m^2
D_h	diffuse irradiance on a horizontal plane, W/m^2
D_t	diffuse irradiance on the PV generator plane, W/m^2
D_{cs}	circumsolar diffuse irradiance, W/m^2
D_{hz}	horizon diffuse irradiance, W/m^2
D_{iso}	isotropic diffuse irradiance, W/m^2
F_{sh}	shading factor
f_{sb}	direct shading factor
f_{sd}	diffuse shading factor
f_{sr}	reflected shading factor
G_h	global irradiance on a horizontal plane, W/m^2
G_t	global irradiance on the PV generator plane, W/m^2
$G_{t,sh}$	global irradiance on a shaded PV generator plane, W/m^2
$\Delta G_{t,sh}$	global irradiance loss caused by shading, W/m^2
x_g, y_g, z_g	topographic coordinates of a PV generator, m
$x_{ob}^i, y_{ob}^i, z_{ob}^i$	topographic coordinates of obstacles, m
I_h	irradiation on a horizontal plane, $W\,h/m^2$
I_t	irradiation on a PV generator plane, $W\,h/m^2$
$I_{t,sh}$	irradiation on a shaded PV generator plane, $W\,h/m^2$
$\Delta I_{t,sh}$	irradiation loss due to shading, $W\,h/m^2$
β	PV generator inclination, rad
γ_{ob}	obstacle altitude angle, rad
$\Gamma_{ob,\,i}$	obstacles' outline functions, rad
γ_s	sun altitude angle, rad
δ	declination of the sun, rad
ϕ	latitude, rad
θ_s	angle of incidence on a PV generator plane, rad
θ_{zs}	angle of incidence on the horizontal plane, rad
ρ	ground albedo
ψ_{ob}	obstacle azimuth angle, rad
ψ_s	sun azimuth angle, rad

for estimating the amount of solar irradiance received on the plane of the PV generator with shading have been reported [4–8]. Most of these methods were based on describing the reduction of irradiation seen from a particular observer point on the PV generator plane, where the shading outline is considered by a space angular description of the horizon reduction, caused by the surrounding obstacles. The shading geometry can be recorded using simple optical measurements or by means of photography, either applying a spherical lens or several photographs from a camera.

As the space angular approach is always valid for a particular position on the PV generator, it is mainly suited for the estimation of the reduction of the irradiation during a longer time period. There are also a number of software tools such as *Sombrero* [9], *Shading* [10], and *TRNSDH* [11] that can be used to estimate mutual shading with polygon projections. However, descriptions of the surroundings using these computer models are quite difficult, and an exact description of irregular objects, such as trees or other plants, is not possible in most cases.

As an alternative, a new method for estimating the irradiance at any time and any point on the PV generator plane has been proposed by the authors. A survey of the surroundings is based on the reading of the topographic coordinates by means of a teodolite. The novelty of this method is its simplicity in determining the obstacles' outline by the use of a set of linear functions in the bi-dimensional coordinate system (azimuth and altitude angle). In addition, this method provides a significant precision in the calculation of instantaneous values of the solar radiation.

In this paper we present the principle of this method and the algorithm developed for estimating the irradiance and the shading factor. The validation of this method on a concrete GC-PV system is also presented.

2. Method for surveying the obstacles' outline

One of the primordial stages in estimating irradiance on a shaded PV generator is a survey of all objects/obstructions that can be found in its surroundings, such as: trees, buildings etc. In fact, the survey must exclusively determine the shadow caused by neighbouring objects only with all distant objects removed. This is done by carrying out a photographic sweep from East to West using a camera, in order to record a sequence of photographs for the PV generator surroundings. This allows us to choose the significant points of all shading objects. Thereafter, we proceed to the reading of topographic coordinates (abscissa, ordinate, altitude) for all significant points of the obstacles $(x_{ob}^i, y_{ob}^i, y_{ob}^i)$ and only one reference point of the PV generator (x_g, y_g, z_g), by means of a well-placed teodolite. Coordinates of other points on the generator with respect to the reference point (x_g, y_g, z_g) can be obtained by applying appropriate geometric transformations. Knowledge of the generator dimensions is necessary here.

Fig. 1 presents an example of a PV generator and its surroundings. Once all of the points characterizing the obstacle outline are obtained, a transformation of these from three-dimensional cartesian coordinates system $(x_{ob}^i, y_{ob}^i, y_{ob}^i)$ into a bi-dimensional coordinate system (azimuth angle ψ_{ob}^i and altitude angle γ_{ob}^i) is made. Geometrical transformations lead to the equations given below. The azimuth angle can be calculated as follows:

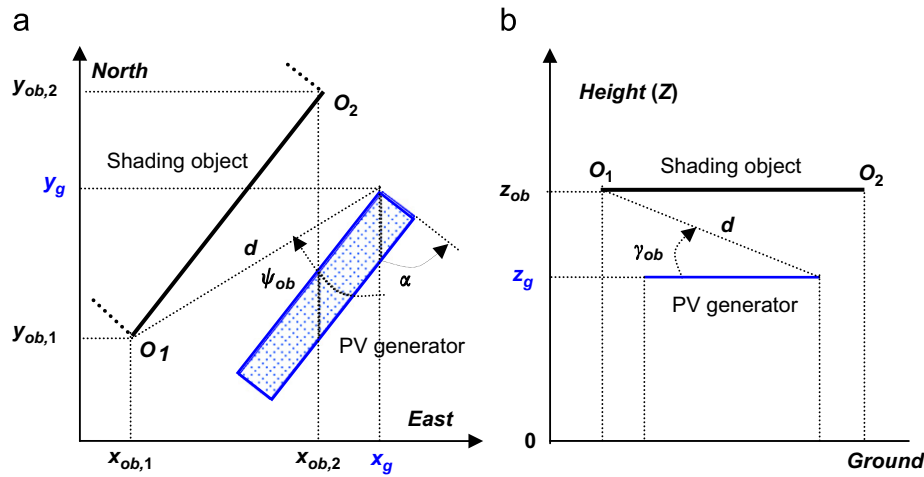$$\psi_{ob}^i = \arctan\left(\frac{x_{ob}^i - x_g}{y_{ob}^i - y_g}\right), \tag{1}$$

Fig. 1. Topographic coordinates of the shading object (x_{ob}, y_{ob}, z_{ob}) and the reference point of the PV generator (x_g, y_g, z_g). The PV generator is faced with an angle α towards the east from the south.
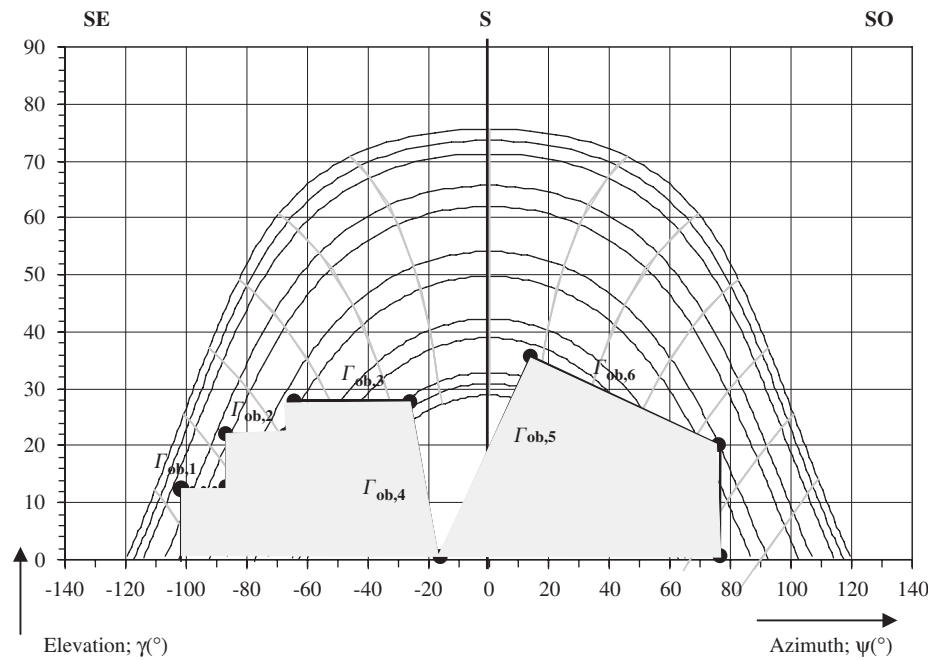

Fig. 2. Example of an arbitrary obstacle outline approximated by linear functions ($\Gamma_{ob,i} = a\psi + b$), displayed on the sun trajectories diagram.

and the altitude angle can be calculated as follows:

$$\gamma_{ob} = \arctan\left(\frac{z_{ob} - z_g}{d}\right), \tag{2}$$

where (ψ^i_{ob}, γ^i_{ob}) are the azimuth and the altitude angles, respectively, of the considered obstacle points, d is the distance in the horizontal plane (east-north) between the PV generator point and every point of the obstacle. It can be calculated as follows:

$$d = \sqrt{(x^i_{ob} - x_g)^2 + (y^i_{ob} - y_g)^2}. \tag{3}$$

Based on the assumptions that the obstacle outline can be assimilated as a polygon of n vertices, this can be

approximated by a set of linear functions described by the following relationship:

$$\Gamma_{ob,i} = \underbrace{\frac{\gamma^{i+1}_{ob} - \gamma^i_{ob}}{\psi^{i+1}_{ob} - \psi^i_{ob}}}_{a}\psi + \underbrace{\frac{\gamma^i_{ob}\psi^i_{ob} - \gamma^{i+1}_{ob}\psi^i_{ob}}{\psi^{i+1}_{ob} - \psi^i_{ob}}}_{b}, \tag{4}$$

where i 1, 2,...$n-1$ is the number of the points, a the function slope and b the second term.

As an example, Fig. 2 illustrates the outline of an arbitrary shading object approximated by linear functions ($\Gamma_{ob,i}$) and superimposed on the sun's trajectory map.

3. The shading factor

In order to estimate the irradiance impinging on the shaded PV generator plane, a dimensionless parameter, known as the shading factor, defined as the fraction of the solar radiation intercepted by surrounding obstacles is used. It actually represents the ratio between the irradiance loss and the global irradiance for an unshaded PV generator. This can be given by the following equation:

$$F_{sh} = \frac{\Delta G_{t,sh}}{G_t}, \tag{5}$$

where $G_{t,sh}$ is the total irradiance received on a shaded PV generator and $\Delta G_{t,sh}$ represents the irradiance loss due to shading.

The calculation of the shading factor requires knowledge of the total irradiance received on unshaded PV generator G_t, and a description of its surroundings' outline using Eq. (4). In the next section, the calculations of the irradiance on both unshaded and shaded planes are treated separately.

3.1. Irradiance on an unshaded PV generator plane

Several models have been developed, of varying complications, as basis for calculating the global irradiance on tilted planes G_t. The differences are largely due to the way that the diffuse terms are treated. The simplest model is based on the assumptions that the sky is isotropic [12], i.e. the radiation on tilted planes includes three components: beam, isotropic diffuse and solar diffuse radiation. This model leads to a substantial underestimation of G_t. However, an improvement of the Liu and Jordan [12] model has been carried out by considering the sky as anisotropic. In this, the circum solar diffuse and/or horizon brightening components have been taken into account. In this context, the most developed model is the well-known *HDKR* (referred to as Hay, Davies, Klucher and Reindl model), which represents the combined model [13]. Also, another model based on a detailed analysis of the three diffuse components has been proposed by Perez et al. [14].

The Perez et al. model performs slightly better than the others. It considers that the sky dome is geometrically divided into three zones acting as diffuse radiation sources: a circumsolar region, a horizontal band and the rest of the celestial hemisphere.

The total solar irradiance on a tilted plane can be evaluated as the sum of the direct beam, the sky diffuse and the ground-reflected components. It can be written as follows:

$$G_t = B_t + D_t + R_t, \tag{6}$$

where B_t and D_t are the direct and diffuse irradiances on a tilted plane, respectively, and R_t is the ground-reflected diffuse component.

The direct irradiance B_t on the tilted plane can easily be obtained from the direct irradiance on horizontal plane B_h using

$$B_t = B_h \left[\frac{\max(0, \cos\ \theta_s)}{\cos\ \theta_{zs}} \right], \tag{7}$$

where θ_s is the angle of incidence of sun's ray radiation on the horizontal plane or the zenithal distance of the sun and θ_{zs} the angle of incidence between the sun's ray and the normal to the tilted surface.

According to the Perez model, the equation used to determine the diffuse irradiance on tilted plane is as follows:

$$D_t = D_{cs} + D_{hz} + D_{iso}, \tag{8}$$

where D_{cs} is the circumsolar diffuse component, D_{hz} the horizon brightening diffuse component and D_{iso} the isotropic diffuse component.

The detailed expression of diffuse components is determined from the diffuse irradiance on the horizontal plane D_h. It is described as follows:

$$D_t = D_h \left(F_1 \frac{\max(0, \cos\ \theta_s)}{\cos\ \theta_{zs}} \right) + D_h(F_2 \sin\ \beta)$$
$$+ D_h \left((1 - F_1) \frac{(1 + \cos\ \beta)}{2} \right), \tag{9}$$

where β is the angle of inclination and F_1, F_2 and F_3 are the anisotropic factors of the diffuse components in the Perez et al. model.

The ground-reflected irradiance R_t is affected by the ground albedo ρ and the surrounding scenery. The reflectivity of the ground is rather low. Consequently, the contribution of the albedo falling on the plane is generally small. It is assumed that the ground is horizontal and of infinite extent and that it reflects isotropically. On this basis, the ground-reflected irradiance on the tilted plane is given by

$$R_t = (1 - \cos\ \beta) \frac{\rho}{2}, \tag{10}$$

If the value of ρ is unknown, it is common to consider that $\rho = 0.2$.

3.2. Irradiance on a shaded PV generator plane

The method proposed for evaluating the irradiance on a shaded plane consists in quantifying the reduction (irradiance loss) $\Delta G_{t,sh}$ due to shading in the total irradiance. As a dimensionless parameter, this irradiance loss can be defined as the shading factor F_{sh}, given by Eq. (1).

The expression for calculating the irradiance on the shaded plane is

$$G_{t,sh} = G_t - \Delta G_{t,sh} \quad \text{or} \quad G_{t,sh} = (1 - F)G_t. \tag{11}$$

If $F_{sh} = 0$, this means that the plane is free from shadows ($\Delta G_{t,sh} = 0$) and if $F_{sh} = 1$, this means that the plane is totally shaded ($G_{t,sh} = 0$).

As the total irradiance on the tilted plane represents the sum of the three components. direct, diffuse and reflect, to calculate the irradiance loss $\Delta G_{t,sh}$, it is necessary to proceed to the determination of the reduction (loss) inherent to each component of the total irradiance. For this purpose, we have introduced three parameters or shading factors f_{sb}, f_{sd} and f_{sr} related to the direct, diffuse and ground-reflected components, respectively. Each one of these represents the shading loss inherent to its component. Therefore, $\Delta G_{t,sh}$ can be written as a weighted function of the collective irradiance components:

$$\Delta G_{t,sh} = f_{sh,b} B_t + f_{sh,d} D_t + f_{sh,r} R_t. \tag{12}$$

On the other hand, in order to quantify the values of these shading factors, we just have to superimpose the sun's trajectories map on the obstacle outline, and examine the position of the sun with respect to the obstacle outline. If the sun's position is inside the obstacle outline, it means that the receiving plane might be completely or partially shaded; otherwise it is free from shadows. The expressions for calculating the three shading factors f_{sb}, f_{sd} and f_{sr} are described later.

The position of the sun in the sky is specified by two solar angles, the solar zenith angle and the solar azimuth angle. The zenith angle γ_s is the angle between the vertical and the line to the sun. The solar azimuth angle ψ_s is the angle between the local meridian and the projection of the line of sight of the sun onto the horizontal plane. We determine the sun position for a certain date, time and geographical data using the well-known equations

$$\psi_s = \arccos\left(\frac{\cos \vartheta_{zs} \sin \phi - \sin \delta}{\sin \vartheta_{zs} \cos \phi}\right), \tag{13}$$
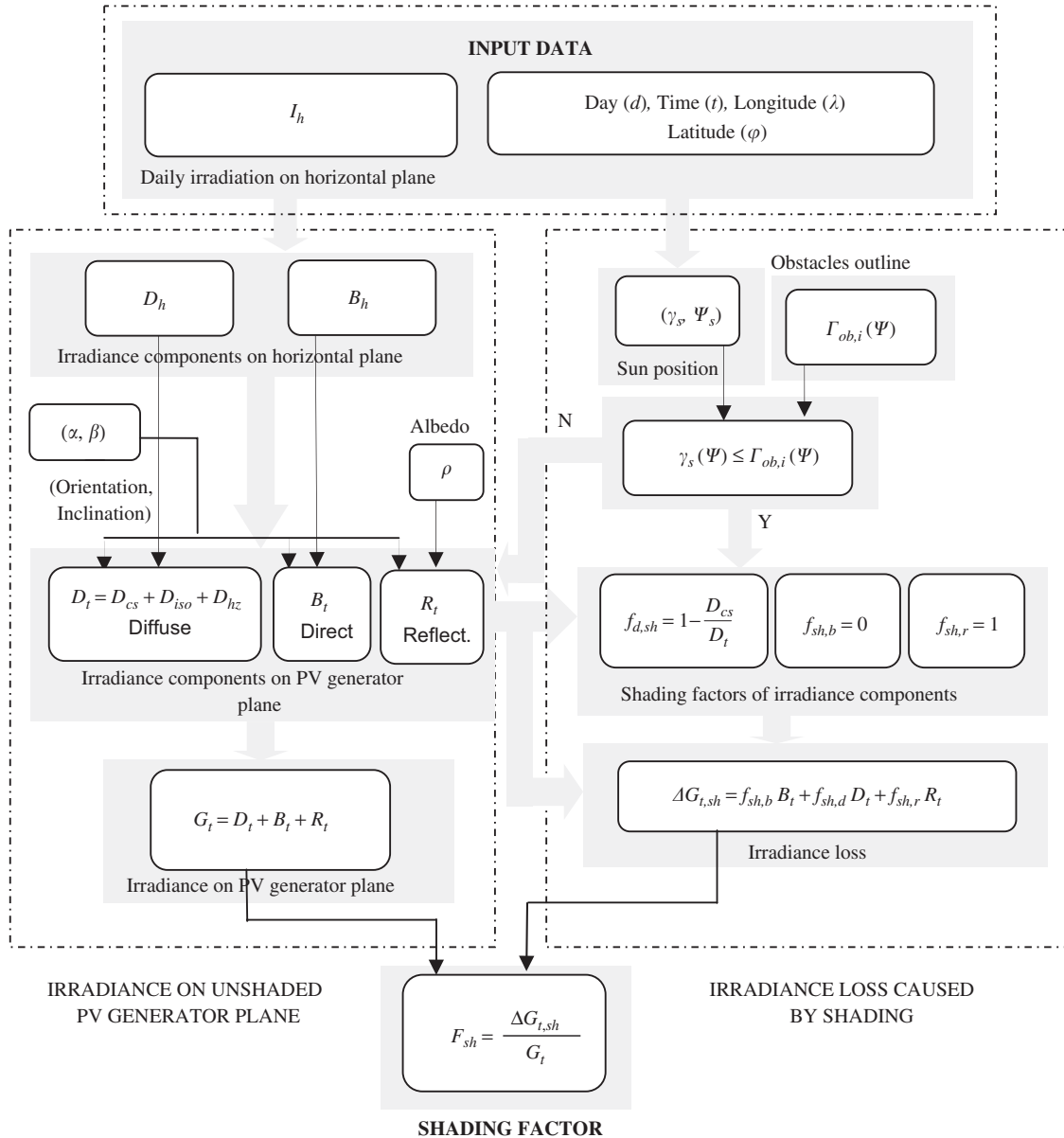

Fig. 3. Flowchart of the algorithm for estimating the shading factor.

$$\gamma_s = \arcsin(\cos\psi_s), \tag{14}$$

where θ_{zs} is the incidence angle of solar radiation on horizontal or zenithal distance of the sun, δ the sun declination and ϕ the latitude of the location.

As previously mentioned, to estimate the three shading factors, we examine the position of the sun with respect to the area delimited by the obstacle outline. If $\gamma_s(\psi) \leqslant \Gamma_{ob}(\psi)$, the direct irradiance is zero, otherwise the direct irradiance is equal to the direct irradiance on the unshaded PV generator. Therefore, the direct shading factor can be written as follows:

$$f_s = \begin{cases} 0 & \text{if} \quad \gamma_s(\psi) \leqslant \Gamma_{ob}(\psi), \\ 1 & \text{otherwise.} \end{cases} \tag{15}$$

However, Eq. (15) is only valid for opaque objects. For semi-transparent objects such as trees, we have to take into account the transmission degree of these objects.

Similarly, if $\gamma_s(\psi) \leqslant \Gamma_{ob}(\psi)$, the diffuse irradiance is partly reduced. In this case, the circumsolar component should be removed from the diffuse irradiance. Hence, the shading diffuse factor can be expressed as follows:

$$f_{sh,b} = \begin{cases} 1 - \dfrac{D_{cs}}{D_t} & \text{if} \quad \gamma_s(\psi) \leqslant \Gamma_{ab}(\psi), \\ 1 & \text{otherwise.} \end{cases} \tag{16}$$

Concerning the shading reflected diffuse component, we note that this component is not affected by the shading. Hence, the shading reflected diffuse component is always equal to 1:

$$f_{sh,r} = 1; \quad \forall \gamma_s(\psi), \tag{17}$$

Based on Eq. (5), we can calculate the daily shading factor using the following equation:

$$F_{sh}^d = \frac{\Delta I_{t,sh}}{I_t}, \tag{18}$$

where I_t is the average daily irradiation on the unshaded PV generator and $\Delta I_{t,sh}$ the daily irradiation loss due to shading.

The irradiance on a partially shaded PV generator and the shading factor calculation process using the proposed method are summarized by the algorithm flowchart of Fig. 3.

4. A case study

In this paper, the GC-PV system studied was installed as a pergola with a capacity of 20 kW$_p$ at the Jaén University campus (37°73′N, 3°78′W) in the South of Spain. This system is an integral part of the GC-PV system of 200 kW$_p$ integrated in the buildings of the Jaén University campus (Fig. 4). The PV array consists of 180 semi-transparent Isofoton I-106 modules, with a total power of 19.08 kW$_p$ at standard test conditions (STC), with a 52° south-east orientation and tilted at 13°. The PV array is divided into 9 sub-arrays of 20 modules each, which are grouped into two
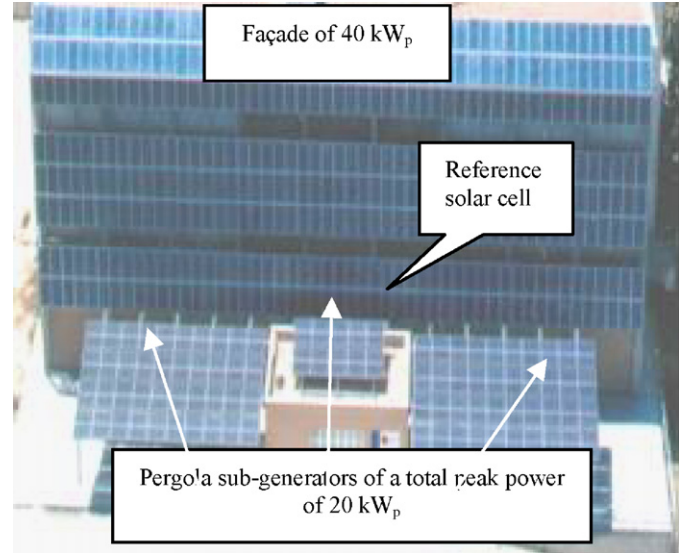

Fig. 4. View of the pergola generator and its surroundings.

parallel strings with 10 modules connected in series per string.

One of the aims of this integrated system was to use the PV array to provide a shady area, very useful in this part of Spain, providing a comfortable outdoor space for students and visitors.

The PV array occupies an area of approximately 154 m^2. It is located near a building which has a GC-BIPV system integrated as a façade with a capacity of 40 kW$_p$ (Fig. 5).

The shading of the PV array-pergola is mainly caused by this neighbouring building. It was observed that the shading on the PV array occurs throughout the year: in the afternoons, early in the summer and late in winter. Fig. 6 shows how the nine sub-arrays were progressively shaded, beginning from the top to the bottom. In order to determine the evolution of the irradiance on the PV array-pergola plane, instantaneous values of 5 min time steps were recorded using a reference cell that was placed beside sub-array SG5.

A survey of the obstacles surrounding the PV array-pergola was performed by means of a teodolite. A record of the topographic coordinates (abscissa, ordinate, altitude) of relevant points on the obstacle (façade) was made, and one point of sub-array SG$_5$ was chosen to serve as the reference for determining the coordinates of all other points on the other sub-arrays. Based on the procedure described, the characterized functions of the obstacles' outline with respect to the central point of each sub-array were determined.

5. Results and discussion

To validate the truthfulness of the proposed method, comparisons between simulated results and real data have been made. Firstly, we started the comparison between the simulated and measured irradiances relative to the
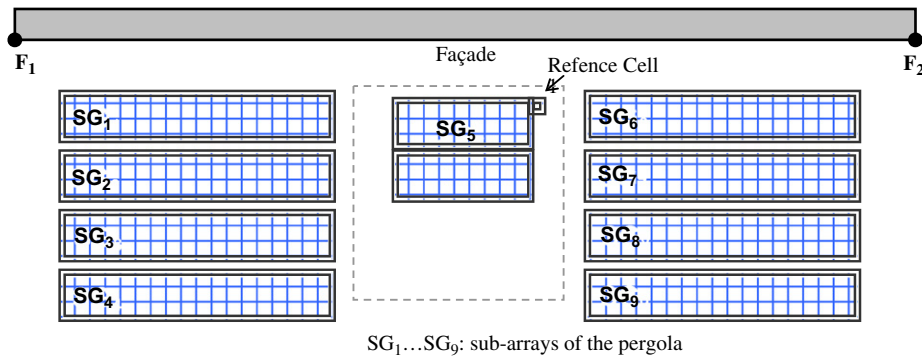
SG$_1$…SG$_9$: sub-arrays of the pergola

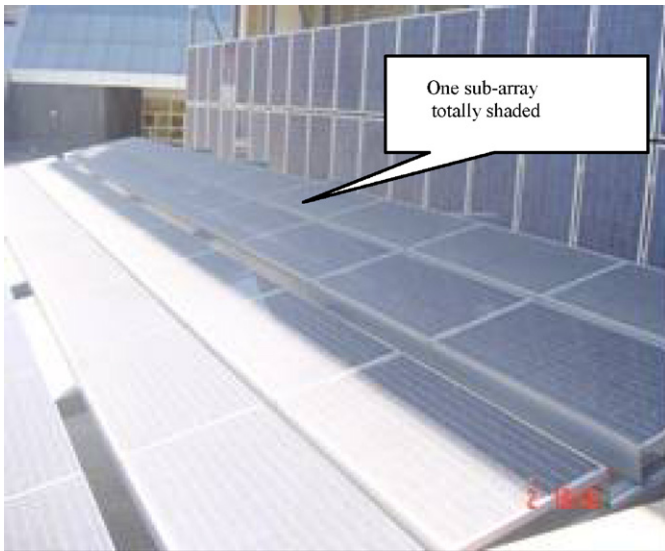Fig. 5. Layout of the pergola surroundings.

Fig. 6. View of the shadow outline on one sub-array of the pergola.

sub-generator SG$_5$, which integrates the reference solar cell, used to measure the irradiance on the same sub-generator.

As a result, Fig. 7 shows the evolution of both measured and simulated values of the irradiance on the sub-generator SG$_5$ on the 2 days 06/06/2005 and 28/09/2005. Also, in this figure, the evolution of the simulated shading factor is presented.

From these results, we can highlight two important points:

• We observe a good agreement between the measured and simulated values of the irradiance. This leads to a preliminary conclusion that the proposed method for estimating the irradiance on shaded photovoltaic generator plane provides a promising estimation of the shading factor and the irradiance.
• The average value of the shading factor, which corresponds to the area delimited by its curve, is significantly larger in autumn than in summer. This can be explained by the fact that the shading varies during the year due to the sun's trajectory across the hemispherical vault.

Secondly, results obtained for others sub-arrays located in different positions were compared. In order to show the inhomogeneity of the solar radiation received on the PV array-pergola, comparisons were made between the simulated values of the irradiance and that measured by a reference cell located beside the sub-array SG$_5$. The results presented in this case are relative to sub-arrays SG$_1$, SG$_4$, SG$_6$ and SG$_9$, which occupy the extreme parts of the pergola (see Fig. 5).

As results, Figs. 8 and 9 show the evolution of both measured and simulated values of the irradiance on the sub-arrays SG$_1$, SG$_4$, SG$_6$ and SG$_9$, together with the simulated shading factor on the 06/06/2005. From these results, it can be noted that:

• The simulated irradiances on both sub-arrays SG$_1$ and SG$_6$ are similar (Fig. 8). The irradiation values obtained were 5.70 kW h/m^2 for SG$_1$ and 5.74 kW h/m^2 for SG$_6$, indicating the same average shading factor of 13.8% (equivalent to an irradiance loss of 0.86 kW h/m^2). In terms of error, this is 2.15% difference between the simulated and measured values.
• The same observations were obtained for sub-arrays SG$_4$ and SG$_9$ with respect to sub-arrays SG$_1$ and SG$_6$. The simulated irradiances on both sub-arrays SG$_4$ and SG$_9$ are similar (Fig. 9). The average values of the irradiation and the shading factor were 5.99 kW h/m^2 and 9.4%, respectively. There is also a good agreement between the simulated and measured values from sunrise until 16:10. This indicates that SG$_5$ (reference) is shaded first approximately 40 min before SG$_4$ and SG$_9$.

Based on the same methodology, we have calculated the average monthly values of the shading factor and the irradiation received on the plane of each one of the nine sub-arrays of the pergola. As an indication, Fig. 10 presents the evolution of the average monthly irradiation and the shading factor during the 2 months June and September. This figure shows clearly the variation of these parameters from one sub-array to another. It can be noted that the maximum irradiations are obtained for sub-arrays SG$_1$ and SG$_6$ and the minimum values correspond to sub-arrays SG$_4$ and SG$_9$. Finally, the average annual value of

I_t = **6.61** kWh/m^2, $I_{t,sh}$ = **5.70** kWh/m^2, F_{sh}^d = **0.138**

I_t = **5.71** kWh/m^2, $I_{t,sh}$ = **5.31** kWh/m^2, F_{sh}^d = **0.070**
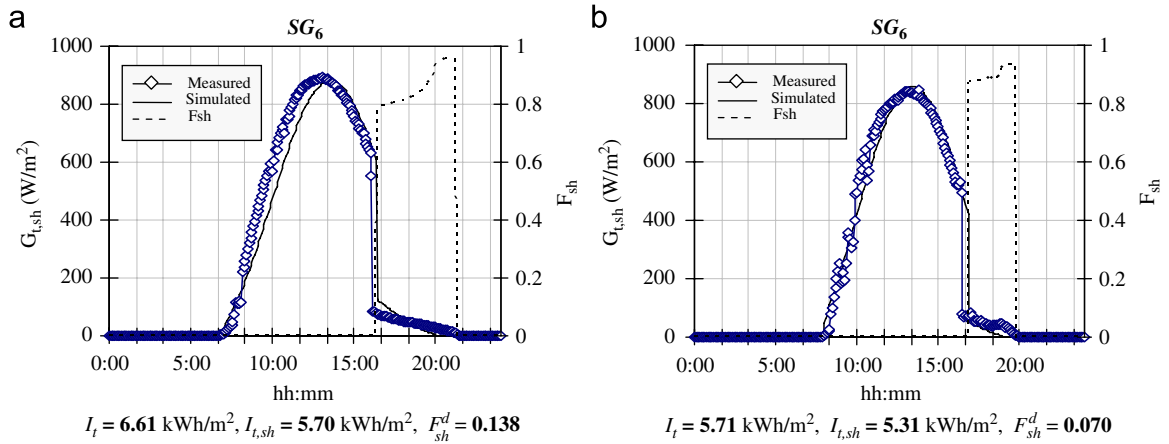
Fig. 7. Evolution of both simulated and measured values of the irradiance received on the sub-array SG$_5$ plane and the shading factor on the 2 days: (a) 06/06/2005 and (b) 28/09/2005.
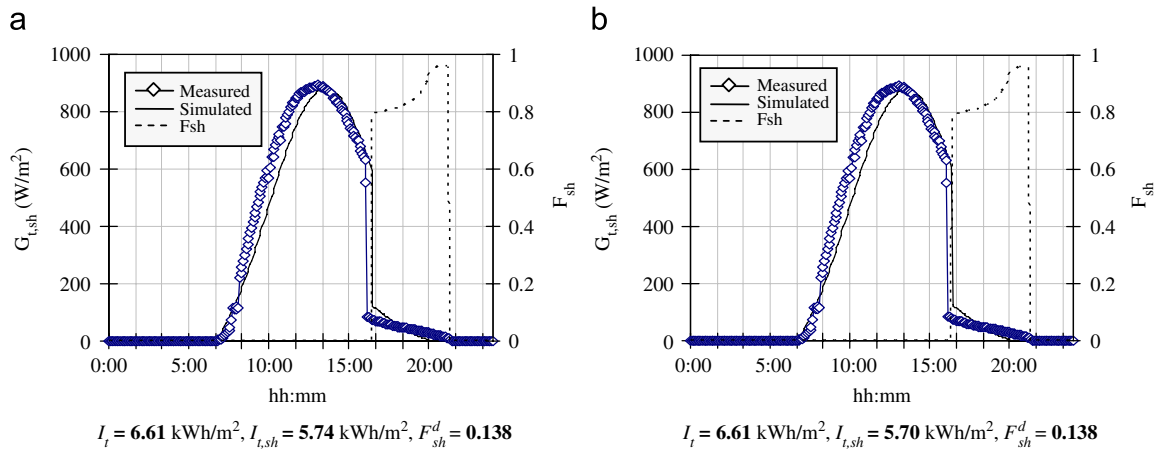

I_t = **6.61** kWh/m^2, $I_{t,sh}$ = **5.74** kWh/m^2, F_{sh}^d = **0.138**

I_t = **6.61** kWh/m^2, $I_{t,sh}$ = **5.70** kWh/m^2, F_{sh}^d = **0.138**

Fig. 8. Evolution of both simulated and measured values of the irradiance received on the sub-generators SG$_1$ and SG$_6$ and the shading factor on 06/06/2005: (a) SG$_1$ and (b) SG$_6$.
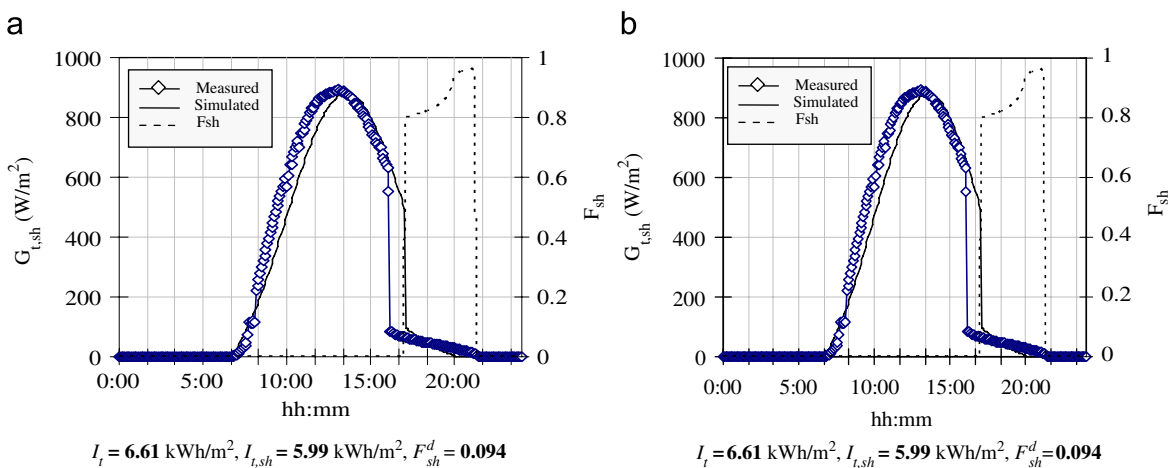

I_t = **6.61** kWh/m^2, $I_{t,sh}$ = **5.99** kWh/m^2, F_{sh}^d = **0.094**

I_t = **6.61** kWh/m^2, $I_{t,sh}$ = **5.99** kWh/m^2, F_{sh}^d = **0.094**

Fig. 9. Evolution of both simulated and measured values of the irradiance received on the sub-generators SG$_4$ and SG$_9$ and the shading factor on 06/06/2005: (a) SG$_4$ and (b) SG$_9$.
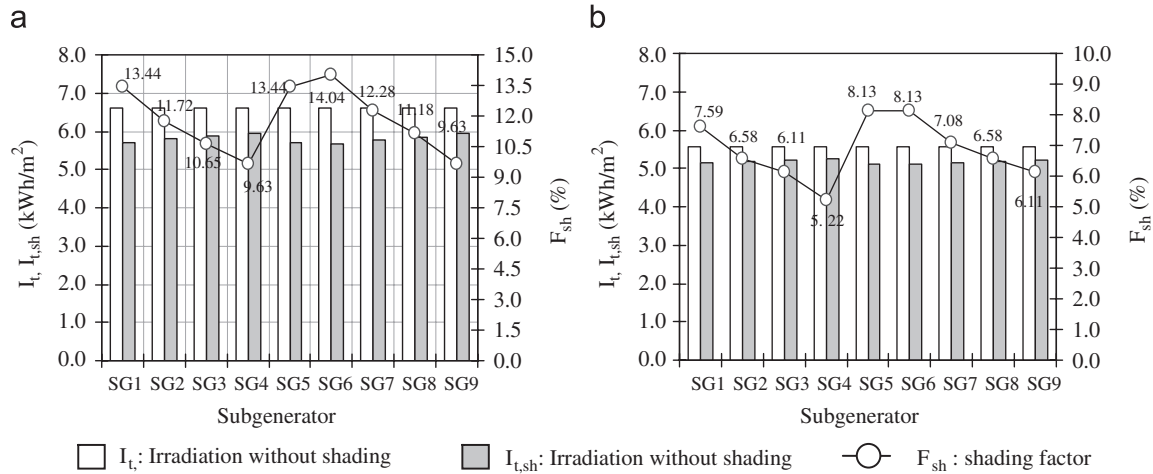
Fig. 10. Values of the simulated irradiations (for June and September) without and with shading and the shading factor for the nine sub-generators (SG$_1$, SG$_2$,…, SG$_9$) of the pergola PV. (a) June and (b) September.

the irradiation received on the plane of the PV array-pergola was 1.631 kW h/m^2, which corresponds to a shading factor of 7.86% (loss due to shading).

6. Conclusions

A new method for estimating the irradiance on partially shaded GC-PV system has been proposed. In this method, a survey of the surroundings based on teodolite reading (topographic coordinates) of only relevant points of the shading objects were done. Then the obstacles' outline was approximated by a set of linear functions. Next, an algorithm for estimating the irradiance and the shading factor (irradiance loss) at any time and any point on the PV array was developed. The calculation of the irradiance was based on the Perez et al. model.

The method was then validated by comparing the simulated and the measured values obtained from a real GC-PV system installation. Preliminary results have shown promising outputs and accuracy of this method.

References

[1] IEA. International Energy Agency report IEA-PVPS T1-14, 2005.
[2] Jahn U, Nasse W. Operational performance of grid connected PV systems on buildings in Germany. Prog Photovoltaics: Res Appl 2004;2:441–8.
[3] Quachning V. On site visits, site surveys and shading analysis. In: Planning and installing photovoltaic systems. James & James publication; 2005. p. 117–31.
[4] Martín EC. Edificios Fotovoltaicos Conectados a la Red Eléctrica. Caracterización y Análisis. PhD thesis, IES, Universidad de Madrid, 1998.
[5] Quachning V, Hanitsh R. Quick determination of irradiance reduction caused by shading at PV-locations. In: Proceedings of the 13th European photovoltaic solar energy conference, 23–27 October 1995, Nice, France, p. 683–6.
[6] Quachning V, Hanitsh R. Irradiance calculation on shaded surfaces. Sol Energy 1998;62(5):369–75.
[7] Woyte A, Nijs B, Belmans R. Partial shadowing of photovoltaic arrays with different system configurations: literature review and field test results. Sol Energy 2003;74:217–33.
[8] Kovach A, Schmid J. Determination of output losses due to shading of building integrated PV arrays using a ray-tracing technique. Sol Energy 1996;57(2):117–24.
[9] Niewinda A, Heidt F. A PC-tools to calculate shadows on arbitrarily oriented surfaces. Sol Energy 1996;58(4–6):253–63.
[10] Shaviv E, Yezioro A. Analyzing mutual shading among buildings. Sol Energy 1997;59:83–8.
[11] Hiller D, Beckman A, Mitchell W. TRNSHD—a program for shading and insolation calculations. Build Environ 2000;35:633–44.
[12] Liu B, Jordan R. The interrelationship and characteristic distribution of direct, diffuse and total solar radiation. Sol Energy 1960;4(3):1–19.
[13] Duffie J, Beckman A. Solar engineering of thermal processes. 2nd ed. New York: Wiley Interscience Publications; 1991.
[14] Perez R, Deals R, Ineichen P, Stewart R, Menicucci D. A new simplified version of the Perez diffuse irradiance model for tilted surfaces. Sol Energy 1987;39(3):221–31.